Noise of Swirling Exhaust Jets

H.Y. Lu,* J.W. Ramsay,* and D.L. Miller*
Boeing Commercial Airplane Company, Seattle, Wash.

Noise and flow characteristics of model swirling jets were measured. A swirling jet from a plug-nozzle generated a strong vortex flow and a broadband noise higher than that of a nonswirling jet. Exit guide vanes were found to be able to decrease the swirl and the noise simultaneously. A swirling jet with a nonswirling jet core flow was tested. The nonswirling core flow prevented the formation of strong vortex and kept the swirling jet noise at a relatively lower level. Noise attenuation for this flow only occurred at small angles from jet axis. The noise increase of the swirling jet over the nonswirling jet was found to depend on swirl angle, pressure ratio, and total temperature of the jet.

I. Introduction

INTEREST in swirling the exhaust flow of an aircraft engine for noise attenuation has been stimulated by Schwartz[1,2] with test results from two different engines. He obtained a ratio of 3 dB overall sound power reduction to 1% of thrust loss for a Pratt & Whitney JT15D-1 (bypass) engine by swirling a part of the primary flow.[1] For a P&WA JT12A-8 turbojet engine, he obtained higher value for this ratio.[2] Most of the noise attenuation, for both engines, occurred at angles less than 50° from the jet axis. The engine exhaust noise with and without swirl vanes was nearly equal in level at higher angles. Although this characteristic provides little in terms of sideline perceived noise level (PNL) suppression, the swirling jet technique may prove to be useful in combination with other noise reduction concepts in a noise suppression system. Therefore, further effort in understanding the flow and noise characteristics of swirling jets is worthwhile.

The noise attenuation presented by Schwartz is based on comparisons of engine exhaust noise with and without swirl vanes. The baseline (without swirl vanes) noise includes jet noise, core engine noise, and possibly swirling jet noise. An engine exhaust flow may have a certain amount of swirl in a certain direction which depends on its operating condition. The change of thrust and noise characteristics of an engine by introducing swirl vanes in the exhaust system should not be considered the same as that of swirling the model jet flow because the model cannot simulate the complicated flow of the full scale engine.

Theoretical work by Tanna[3] showed that the swirling (helical) motion of sources increase noise in the direction normal to the jet axis as the tangential flow (swirl) velocity increases. If the absolute velocity of the jet noise source is kept constant, the swirl motion decreases the axial velocity and decreases the noise in the jet axial direction. Tanna's theoretical model is a close simulation of the behavior of noise sources in a swirling jet.

Since the engine tests conducted by Schwartz showed no increase in noise for the swirling jet over the baseline jet at angles near normal to the jet axis, there is a question whether the baseline jet is free of swirl and core noise. Another approach to test the effect of swirling flow on jet noise is to conduct model tests where the upstream noise and flow disturbances are minimized. The flow and noise characteristics of a swirling jet can be observed and compared with that of a nonwrirling jet.

Bryce and Stevens[4] investigated the noise of an engine exhaust system by a scale model test. They concluded that the measured far-field noise was related to a swirl-strut interaction caused by the upstream flow angle incident on the struts. However, it is believed that in their tests, the struts leave different amounts of downstream swirl flow with different amounts of upstream swirl. Consequently, the measured noise which includes swirl-strut interaction noise, swirl-plug interaction and the swirling jet noise is difficult to decompose into each component.

In the present test, the flow and noise characteristics of swirling jets are investigated with the following model flow configurations: 1) Swirling jet flow from a plug-nozzle; 2) Item 1 with struts (exit guide vanes); 3) Swirling jet flow with a short, blunt (separated flow) plug; 4) Swirling jet with a nonswirling jet core flow.

These model flow configurations were selected to identify the effect of each component on the swirling jet noise. Configuration variations were tested one-at-a-time in order to clearly separate the effect of each component.

II. Test Models and Apparatus

The swirl model system was designed to simulate the primary exhaust configuration of current high-bypass ratio engines. Figure 1 is a sketch of the hardware showing the long and the short (separated flow) plugs. The nozzle exit diameter is 12.7 cm and the plug has a 8.9 cm diameter at the nozzle exit. The model was designed with several removable and interchangeable parts as indicated in Fig. 1 to allow isolation of the effects on exhaust noise including swirling jet noise, strut noise, and separated plug flow noise. Two sets of swirl vanes were used to provide different swirl angles at the exit plane. A yaw probe was used to measure the radial

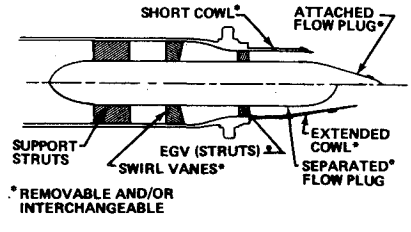

Fig. 1 Model configuration for swirling jet.

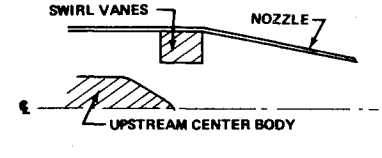

Fig. 2 Model for swirling jet with nonswirling jet core.

Presented as Paper 76-510 at the 3rd AIAA Aero-Acoustics Conference, Palo Alto, Calif., July 20-23, 1976; submitted July 29, 1976; revision received Jan. 6, 1977.
Index category: Aerodynamics.
*Acoustic Engineer.

distributions of the swirl angle, total pressure and total temperature in the jet. The static-pressure distribution along the plug was recorded. Oil trace (traces of the flow of an oil film) on the plug surface was used to indicate flow separation and shadowgraphs were used to detect shock wave formation.

Acoustic data were taken in the Boeing Large Anechoic Chamber (22.9 m wide, 19.8 m long and 9.15 m high). Room ambient conditions are maintained by inducing ventilation air with negligible wind speed. Far-field microphones were placed on a 7.6 m radius polar array from 70° to 160° from inlet axis. Near-field microphones were arranged along a line approximately 20 cm from the nozzle exit center and at an angle of 10° to the jet centerline.

For the test of a swirling jet with a nonswirling jet core, the model shown in Fig. 2 was used. The nozzle exit diameter is 8.38 cm. The annular swirl vanes has an inner diameter of 7.6 cm and an outer diameter of 11.4 cm. The swirl vanes were 60° circular arcs with leading edges at 0° angle of attack. A yaw probe was used for the survey of the flow field. Acoustic data were taken by sideline microphones from 90° to 160° from the inlet axis. Sideline arrays were located at 0.61 m and 4.36 m from the jet centerline.

III. Test Results

Effect of Swirl with a Plug-Nozzle

The tests were run with pressure ratios (PR) from 1.1 to 1.5 and total temperatures (T_T) of ambient and 810K. Two sets of swirl vanes provided swirl angles of 9° and 18° respectively at the nozzle exit without the exit guide vanes (EGV's). The measured swirl angle distribution at the end of the plug is shown in Fig. 3 for the 18° nozzle exit swirl angle where R_j is the nozzle radius. A large increase of swirl angle toward the center of the jet at the end of plug is caused by the decrease of plug diameter. A tornado type vortex occurred near the center of the jet. Figure 4 is a plot of static-pressure distribution along the plug. The static-pressure is effected by two different mechanisms. For a nonswirling or very weakly swirling jet, the static-pressure increases slightly along the plug due to the diffusion effect from the plug (subsonic flow). Although a slight adverse pressure gradient existed along the plug, the oil trace showed no separation. For a moderate swirling jet, the decrease of plug diameter causes the formation of a strong vortex since the plug surface friction is negligible and the angular momentum of the jet is conserved. At pressure ratio 1.5 the static-pressure near the end of the plug dropped to 5.7 $\times 10^4$ N/m^2 ($\approx$0.57 atm). The favorable pressure gradient along the plug kept the boundary layer relatively thin and the local flow was accelerated to a supersonic condition. This is verified by the formation of a shock wave downstream of the plug as shown in the shadowgraph of Fig. 5. The existence of the shock wave provided a part of the recovery of local static-pressure for the downstream swirling jet flow.

The noise of the swirling jet from a plug-nozzle was found to be much higher than that from the same configuration but without swirl. Figures 6 and 7 show the overall SPL polar distributions. Suppression can only be found for the case of a hot jet in an angular region less than 40° from jet axis which is not an important region for noise suppression. At other angles, the noise increase due to swirl is substantial. Figure 8 shows the noise spectra at 110° relative to the inlet axis. The swirl jet noise spectra have the same broadband nature of jet noise.

Both the noise level and the peak frequency increase with the exit swirl angle. The increase in high-frequency noise level at angles close to normal of jet axis is particularly significant because it will cause an increase in perceived noise level over the nonswirling jet. The dependence of swirling jet noise on

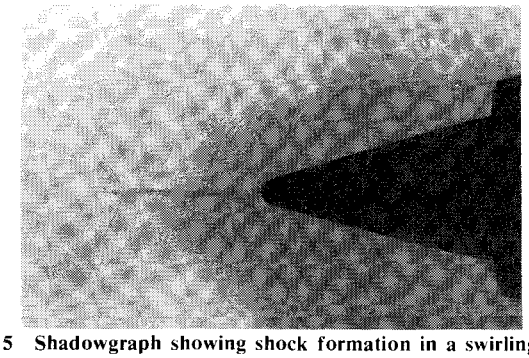

Fig. 5 Shadowgraph showing shock formation in a swirling jet of pressure ratio 1.5 (lines darkened for reproduction purposes.)

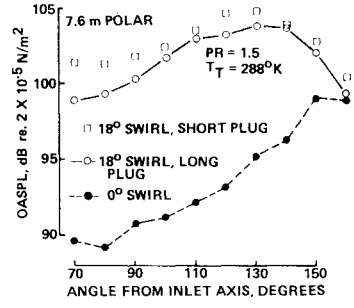

Fig. 6 OASPL for swirling and nonswirling cold jets.

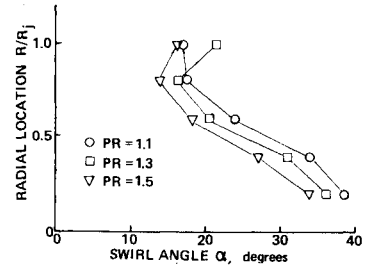

Fig. 3 Swirling angle at the end of plug.

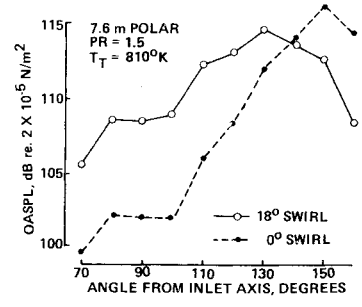

Fig. 7 OASPL for swirling and nonswirling hot jets.

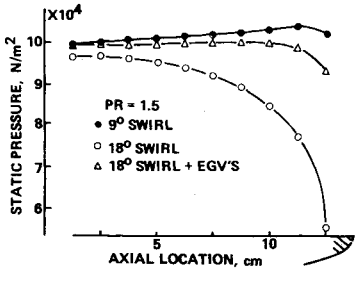

Fig. 4 Static pressure along the plug.

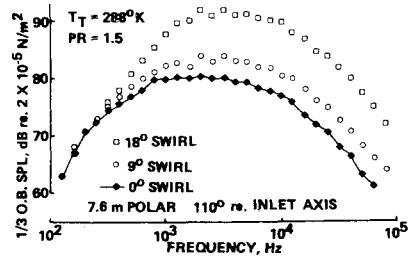

Fig. 8 Swirling jet noise spectra.

the pressure ratio and total temperature is shown in Fig. 9. The peak ΔSPL is defined as the peak ⅓-octave band SPL with the swirl minus the peak ⅓-octave band SPL baseline under the same operating condition. The dependence shows the change in noise generation (source) strength between a swirling and nonswirling jet.

Effects of Struts and Separated Flow Plug

The struts or EGV's are symmetric airfoils which were axially aligned in the model system shown in Fig. 1. The EGV's reduce the swirl angle by more than 50% at the nozzle exit. In the case of pressure ratio 1.5, for example, the exit swirl angle dropped from 18° to 7°. The corresponding static-pressure along the plug is shown in Fig. 4. The strength of the vortex was reduced and no shock waves were found in the shadowgraphs.

Figure 10 shows the noise spectra with and without EGV's. The interaction between the swirling flow and the EGV's is one of the potential noise source mechanisms, but it was not separated from the swirling jet noise in this experiment. The large decrease in noise which accompanied the EGV's indicated that the swirling jet noise is dominant. Since the EGV's reduce the swirl angle, a reduction of peak swirling jet noise of 7 dB for a pressure ratio 1.5 flow is shown in Fig. 10. At pressure ratio 1.1, an SPL reduction of 10 dB was found in the frequency range of 2000 to 50 000 HZ, while no reduction was found at 200 Hz and 80 kHz.

A short, blunt, separated flow plug (Fig. 1) was used to test the noise due to flow separation from the plug in the presence of swirl. The flow separation increases the noise by 1 to 3 dB as shown in Fig. 6. Spectra at 110° from inlet axis showed almost a uniform 1 to 2 dB difference, throughout the measured frequency range, between the noise of the short plug and the long plug configurations.

Swirling Jet With a Nonswirling Jet Core

In order to prevent the formation of a strong vortex due to the combination of the plug-nozzle and the swirling exit flow, a nonswirling jet core flow was introduced. The model shown in Fig. 2 was tested at pressure ratios of 1.2, 1.4, and 1.8, at total temperatures of ambient and 556 K.

Yaw probe measurements were taken at the nozzle exit (x = 0) and at two nozzle diameters downstream ($x = 2D_j$).

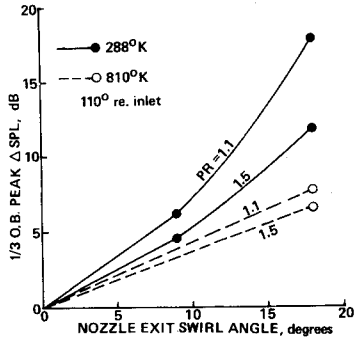

Fig. 9 Swirling jet noise increase.

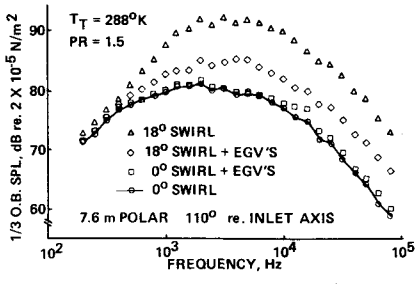

Fig. 10 Spectra with and without exit guide vanes.

The swirl angle radial distribution for pressure ratio 1.4 is shown in Fig. 11. (R_j is the nozzle radius). Close to the edge of the nozzle exit, the swirl angle is 29° for $PR = 1.2$ and 24° for $PR = 1.8$. The swirl angle distributions at two nozzle diameters downstream were found to be nearly the same for the pressure ratios and total temperatures tested. Figure 12 shows the dimensionless abolute velocity distributions at $x = 2D_j$. The jet half-spread angle for 10% velocity line is approximately 9° which is larger than 5.7° of an equivalent nonswirling jet. The static-pressure drop ($p_a - p$) is given in Fig. 13, which shows that near the jet core the static-pressure is 2.34×10^3 N/m^2 (≈ .023 atm) lower than that of the ambient pressure.

Noise spectra at 110° from inlet axis of the swirling and the nonswirling jets of the same nozzle are given in Fig. 14. The

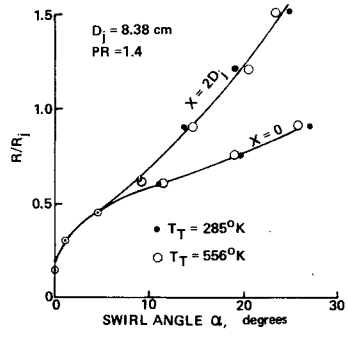

Fig. 11 Swirl angle distribution.

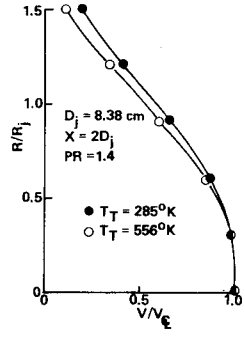

Fig. 12 Velocity distribution.

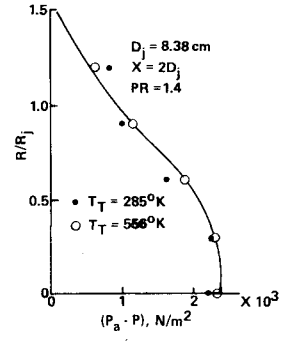

Fig. 13 Static pressure drop.

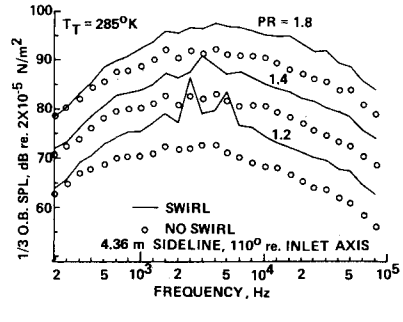

Fig. 14 Spectra of cold swirling jets with nonswirling jet core.

data clearly show that a swirling jet generates more noise than a nonswirling jet at the same pressure ratio. At ambient total temperature and a pressure ratio 1.2, a tone of 2500 Hz and its second harmonic 5000 Hz appeared in the spectrum. The tone source was not positively identified. The centerbody and the annular ring of the swirl vanes may have caused the whistling sound.

Figure 15 shows the spectra for hot jets with a total temperature of 556 K. The difference in SPL between the swirling jet and the nonswirling jet is less than that of ambient total temperature case. This trend is consistent with the previous result of swirling jet from a plug-nozzle. The whistle tone in this case is not so outstanding as in the case of ambient total temperature. It can be identified in Fig. 15 for pressure ratio 1.2. The tone seemed to be submerged into the ⅓-octave band level for higher pressure ratios. Under this condition, the tone has nearly no influence in OASPL. The OASPL distributions along the 4.36 m sideline for the hot jets are given in Fig. 16. The OASPL for the case of ambient total temperature is influenced by the tone, particularly for pressure ratio 1.2. For both hot and cold flow, the swirling jet with a nonswirling jet core has a smaller noise increase at large angles from the jet axis than that of a plug-nozzle. The decrease in noise is due to the absence of local flow acceleration in the nonswirling jet core. Attenuation of jet noise can be found at angles less than 40° from jet axis.

IV. Estimation of Thrust Loss

The thrust loss was not measured during the tests. The following analysis was made to estimate the thrust loss of a swirling jet with a nonswirling jet core.

In order to compare the thrust between a swirling jet and a nonswirling jet, a set of conditions has to be defined as a base of comparison. It is practical and meaningful to compare the thrust under the condition of equal total pressure, equal total temperature and equal mass flow rate. This set of conditions will imply equal fuel consumption but not equal nozzle exit diameter.

The mass flow rate $\dot{m}$ and the thrust F of a subsonic swirling jet with a nonswirling jet core are

$$\dot{m}=\pi r_i^2\rho_i v_i+2\pi\cos\alpha\int_{r_i}^{r_0}\rho v r dr \tag{1}$$

$$F=\pi r_i^2[\rho_i v_i^2+(p_i-p_a)]$$

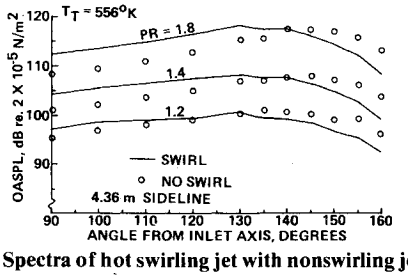

Fig. 15 Spectra of hot swirling jet with nonswirling jet core.

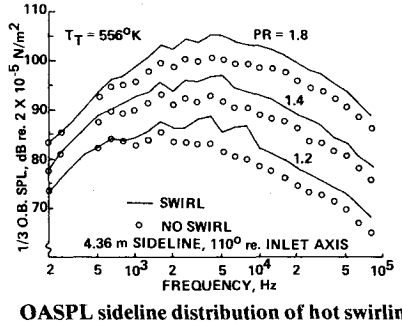

Fig. 16 OASPL sideline distribution of hot swirling jets.

$$+2\pi\int_{r_i}^{r_0}[\rho v^2\cos^2\alpha+(p-p_a)]rdr \tag{2}$$

where r_i is the nonswirling jet core radius, r_0 is the swirling jet nozzle radius, ρ is density, v is absolute velocity, p is static pressure. p_a is the ambient pressure. Subscript i denotes constant core condition. α is the swirl angle assumed constant at nozzle exit.

For the same mass flow rate, an equivalent nonswirling subsonic jet has a nozzle exit radius r_c. It is found, by using ideal gas and isentropic condition, that

$$r_c^2=\left\{\left[\left(\frac{p_i}{p_t}\right)^{\frac{2}{\gamma}}-\left(\frac{p_i}{p_t}\right)^{\frac{\gamma+1}{\gamma}}\right]^{1/2}r_i^2+2\cos\alpha\int_{r_i}^{r_0}\left[\left(\frac{p}{p_t}\right)^{\frac{2}{\gamma}}-\left(\frac{p}{p_t}\right)^{\frac{\gamma+1}{\gamma}}\right]^{1/2}rdr\right\}\Bigg/\left[\left(\frac{p_a}{p_t}\right)^{\frac{2}{\gamma}}-\left(\frac{p_a}{p_t}\right)^{\frac{\gamma+1}{\gamma}}\right]^{1/2} \tag{3}$$

where p_t is the total pressure and $\gamma=c_p/c_v=1.4$ is the ratio of specific heats.

The ratio of the thrust F of the swirling jet to the thrust F_c of nonswirling jet is

$$\frac{F}{F_c}=\frac{A+B}{\left[\left(\frac{p_a}{p_t}\right)^{\frac{1}{\gamma}}-\left(\frac{p_a}{p_t}\right)\right]r_c^2} \tag{4}$$

where

$$A=\left[\left(\frac{p_i}{p_t}\right)^{\frac{1}{\gamma}}-\left(\frac{p_i}{p_t}\right)-\frac{\gamma-1}{2\gamma}\frac{p_a-p_i}{p_t}\right]r_i^2$$

$$B=2\int_{r_i}^{r_0}\left\{\left[\left(\frac{p}{p_t}\right)^{\frac{1}{\gamma}}-\left(\frac{p}{p_t}\right)\right]\cos^2\alpha-\frac{\gamma-1}{2\gamma}\frac{p_a-p}{p_t}\right\}rdr$$

If $\alpha\le 30°$ and $r_0/r_i\le 1.5$, the difference between p_a and p_i is small for subsonic jets. We take the approximation

$$p=(p_a+p_i)/2 \tag{5}$$

to simplify the integration.

The thrust loss is plotted in Fig. 17. The swirling jet with nonswirling core tested in this experiment has an estimated thrust loss of 4%.

Replacing r_c by r_0 in Eq. (4), one finds the thrust loss of a swirling jet based on equal exit diameter. Since $r_0\ge r_c>r_i$, thrust loss based on equal diameter is much higher.

Conclusions

The basic results and findings from these model tests and analysis are: 1) Swirling jet noise is broadband and is similar

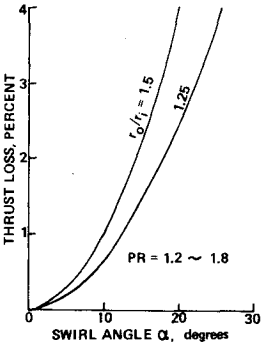

Fig. 17 Calculated thrust loss of a swirling jet.

to nonswirling jet noise. The frequency of the peak level is higher than that of a pure jet. For a plug-nozzle, this noise is caused by the formation of a strong vortex about the plug which results in very high local velocity; 2) Swirling jet noise is higher than nonswirling jet noise at high angles from jet axis. Noise attenuation by swirling the jet flow only occurs at angles less than 40° from the jet axis; 3) The difference between swirling and nonswirling jet noise increases with increasing swirl angle, and decreases with increasing pressure ratio and total temperature; 4) The EGV's reduce the swirl angle and swirling jet noise simultaneously; 5) A nonswirling jet core in a swirling jet can prevent the formation of a strong vortex and reduces swirling jet noise. The swirling jet noise is higher than that of a pure jet; 6) A swirling jet has a larger spread angle than a nonswirling jet; 7) Thrust loss due to jet swirl is not negligible.

It can be concluded that considerable testing of swirling jet flow and noise have to be conducted in order to predict the swirling jet characteristics. Particular emphasis should be given to the understanding of the influence by ambient parallel flow. The present work illustrated some important characteristics of swirling jets. The application of this work to full-scale engines depends on the development of swirling jet noise scaling technology and a detailed knowledge of the full-scale engine exhaust flow characteristics.

References

[1]Schwartz, I.R., "Jet Noise Suppression by Swirling the Jet Flow," AIAA Paper 73-1003, Seattle, Wa., Oct. 1973.

[2]Schwartz, I.R., "Minimization of Jet and Core Noise of a Turbojet Engine by Swirling the Exhaust Flow," AIAA Paper 75-503, Hampton, Va., March 1975.

[3]Tanna, H.K., "On the Effect of Swirling Motion of Sources on Subsonic Jet Noise," *Journal of Sound and Vibration,* Vol. 29, pp. 281-293, Aug. 1973.

[4]Bryce, W.D. and Stevens, R.C.K., "An Investigation of the Noise from a Scale Model of an Engine Exhaust System," AIAA Paper 75-459, Hampton, Va., March 1975.